

# OH-equivalent temperatures derived from ACE-FTS and SABER temperature profiles – a comparison with OH\*(3-1) temperatures from Maynooth (53.2° N, 6.4° W)

F. J. Mulligan<sup>1</sup> and R. P. Lowe<sup>2</sup>

<sup>1</sup>National University of Ireland Maynooth, Maynooth, Co. Kildare, Ireland

<sup>2</sup>The University of Western Ontario, London, Ontario, N6A 3K7, Canada

Received: 16 March 2007 – Revised: 22 February 2008 – Accepted: 13 March 2008 – Published: 13 May 2008

**Abstract.** OH-equivalent temperatures were derived from all of the temperature profiles retrieved in 2004 and 2005 by the ACE-FTS instrument in a 5 degree band of latitude centred on a ground-based observing station at Maynooth. A globally averaged OH volume emission rate (VER) profile obtained from WINDII data was employed as a weighting function to compute the equivalent temperatures. The annual cycle of temperature thus produced was compared with the annual cycle of temperatures recorded at the ground-based station more than a decade earlier from the OH\*(3-1) Meinel band. Both data sets showed excellent agreement in the absolute value of the temperature minimum ( $\sim 162$  K) and in its time of occurrence in the annual cycle at summer solstice. Away from mid-summer, however, the temperatures diverged and reach a maximum disagreement of more than 20 K in mid-winter. Comparison of the Maynooth ground-based data with the corresponding results from two nearby stations in the same time-period indicated that the Maynooth data are consistent with other ground stations. The temperature difference between the satellite and ground-based datasets in winter was reduced to 14–15 K by lowering the peak altitude of the weighting function to 84 km. An unrealistically low peak altitude would be required, however, to bring temperatures derived from the satellite into agreement with the ground-based data.

OH equivalent temperatures derived from the SABER instrument using the same weighting function produced results that agreed well with ACE-FTS. When the OH 1.6  $\mu\text{m}$  VER profile measured by SABER was used as the weighting function, the OH equivalent temperatures increased in winter as expected but the summer temperatures were reduced resulting in an approximately constant offset of  $8.6 \pm 0.8$  K

*Correspondence to:* F. J. Mulligan  
(frank.mulligan@nuim.ie)

between ground and satellite values with the ground values higher. Variability in both the altitude and width of the OH layer within a discernable seasonal variation were responsible for the changes introduced. The higher temperatures in winter were due to primarily to the lower altitude of the OH layer, while the colder summer temperatures were due to a thinner summer OH layer. We are not aware of previous reports of the effect of the layer width on ground-based temperatures.

Comparison of OH-equivalent temperatures derived from ACE-FTS and SABER temperature profiles with OH\*(3-1) temperatures from Wuppertal at 51.3° N which were measured during the same period showed a similar pattern to the Maynooth data from a decade earlier, but the warm offset of the ground values was lower at  $4.5 \pm 0.5$  K. This discrepancy between temperatures derived from ground-based instruments recording hydroxyl spectra and satellite borne instruments has been observed by other observers. Further work will be required by both the satellite and ground-based communities to identify the exact cause of this difference.

**Keywords.** Atmospheric composition and structure (Airglow and aurora; Pressure, density, and temperature; Instruments and techniques)

## 1 Introduction

Inter-comparison of geophysical datasets measured by different techniques is valuable for the validation of the techniques themselves in addition to offering the possibility of uncovering new physical phenomena. The ideal case for such comparisons arises when the measurements are taken at the same time and place. Even under ideal conditions, it can be difficult to reconcile a discordance between datasets which can

occur due to differences in signal levels and instrument characteristics (e.g. Oberheide et al., 2006). On the other hand, She and Lowe (1998) have pointed out that valuable inter-comparison between two instruments at different sites may be achieved on a statistical basis, when the comparison is restricted to parameters which are of large spatial scale and long period.

This study reports on a comparison of temperatures retrieved by two satellite instruments, ACE-FTS and SABER for the period January 2004 to December 2005 with temperatures obtained from the OH\*(3-1) Meinel band which were recorded more than a decade earlier. To facilitate the comparison, we computed an ‘‘OH-equivalent temperature’’ (the temperature that the ground-based instrument would detect for a given temperature profile) for each satellite temperature profile. The study is prompted by the following considerations: (a) validation of the concept of an OH-equivalent temperature together with the near global coverage of the satellites offers the possibility of establishing a global climatology of OH temperatures (see e.g. von Savigny et al., 2004); (b) the extensive latitude coverage of both ACE-FTS and SABER makes them a potentially very valuable resource as a transfer standard for inter-comparison of temperatures obtained by different techniques and from observation stations at different locations; (c) the annual average temperature of the atmosphere in the region of the mesopause has changed very little over the past decade (e.g. Beig et al., 2003); (d) the averaged altitude of emission of the OH Meinel bands has been found to be remarkably consistent (87 km in altitude and a width at half intensity of 8–10 km) (e.g. She and Lowe, 1998; Oberheide et al., 2006) since the seminal report on the topic by Baker and Stair in 1988; (e) the quality and volume of data available in the datasets is sufficient for a useful statistical comparison; (f) similar efforts are currently underway for the results from other ground-based instruments (Oberheide et al., 2006; L3pez-Gonz3lez et al., 2007); (g) temperatures derived from OH emissions are beginning to be used in the study of long term change in the mesosphere and lower thermosphere (Bittner et al., 2002; Sigernes et al., 2003). It is important, therefore, that we have a clear understanding of precisely what such a temperature measures.

## 2 Instruments

### 2.1 Ground-based OH\*(3-1) data

The ground-based data used in this study, some of which have been reported already (Mulligan et al., 1995), were recorded at Maynooth (53.2° N, 6.4° W) over the two-year period 1993 to 1994. Since the Maynooth station did not record any data during the operational phase of either ACE-FTS or SABER, these two years were selected for the study because they have the highest number of individual measurements available, and they match very closely the timeframe

in their phase of the solar cycle. The instrument used to record the data is a Fourier transform infrared spectrometer supplied by Bomem Inc. It records the spectrum in the region 1.0–1.65  $\mu\text{m}$  using a thermoelectrically cooled InGaAs detector and has a maximum resolution of  $2\text{ cm}^{-1}$ . It has a circular field-of-view of approximately  $1.5^\circ$  and an OH\* spectrum with a signal-to-noise ratio sufficient to recover the rotational temperature to within an uncertainty of less than  $\sim 5\text{ K}$  is acquired in approximately 5 min. The  $P_1(2)$ ,  $P_1(3)$  and  $P_1(4)$  lines in the (3,1) band in each spectrum were used to derive temperatures because they are among the most intense lines in the spectrum and are not affected to any significant extent by water vapour absorption (Turnbull and Lowe, 1983). Details of the temperature determination and the transition values used are given in Mulligan et al. (1995).

The instrument was operated on all cloudless nights in the two-year period giving 114 nights in 1993 and 106 nights in 1994. Figure 1 shows the temperatures obtained on the night of 16/17 September 1993 and is a typical night record. On average there are approximately 100 individual temperature measurements per night with up to 160 in the longest winter night and as low as 40 in the shortest summer night. The total number of individual temperature measurements in the two-year period was 21 378. An averaged nightly temperature is calculated for each night, where the contribution of each temperature to the nightly average is weighted according to the inverse-square of its individual measurement uncertainty (Bevington, 1992). Since the comparison reported here is a statistical one, it is important to note the temporal bias in the number of measurements per night, with more measurements in winter than in summer due to the shortness of summer nights. In addition, the time period over which the temperature is averaged in summertime (just over 5 h) is considerably shorter than in winter (typically 14 h). The potential effect of this bias will be considered below.

### 2.2 ACE-FTS data

SCISAT-1 also known as the Atmospheric Chemistry Experiment (ACE) is a Canadian satellite mission designed for remote sensing of the Earth’s atmosphere using occultation spectroscopy (Bernath et al., 2005). It was launched on 13 August 2003 into a circular 650 km orbit with an inclination of  $74^\circ$  to the equator thereby providing for good coverage of tropical, mid-latitude and polar regions. The primary instrument on board the satellite is a Fourier transform spectrometer (FTS) operating between 2 and 13 microns with an unapodized resolution of  $0.02\text{ cm}^{-1}$  which allows the vertical distribution of trace gases, pressure and temperature to be measured. The instrument has a circular field-of-view of 1.25 mrad which determines the vertical resolution to be about 3–4 km in the altitude range 10–150 km. Pressure and temperature as a function of altitude are determined from the FTS measurements through analysis of carbon dioxide absorption (Boone et al., 2005). The altitude spacing is

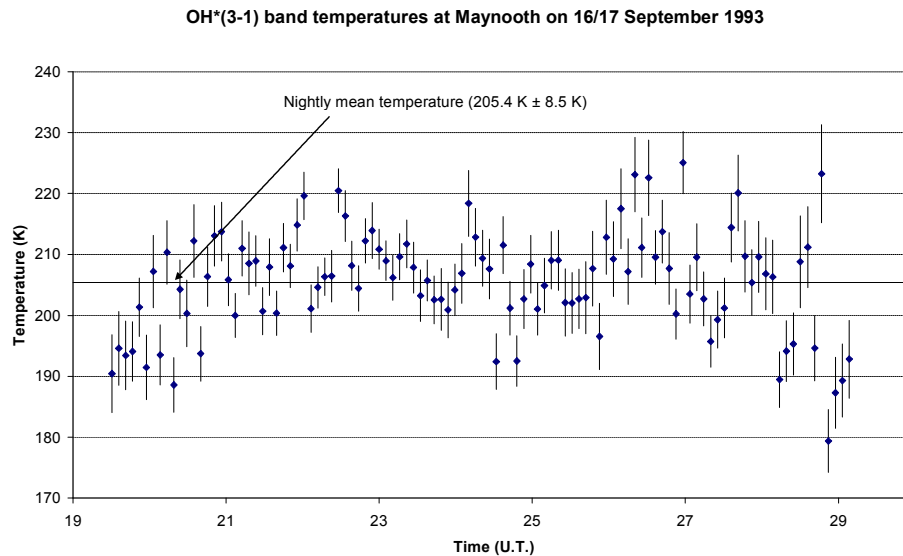


**Fig. 1.** Rotational temperatures calculated from the OH\*(3-1) band recorded at Maynooth (53.2° N, 6.4° W) on the night of 16/17 September 1993, which is a representative night from the two-year dataset.

controlled by the scan time (2 s at full resolution) of the FTS and the orbit of the satellite. It ranges from 2 km for long occultation events (slowly rising/setting sun) (an occultation event is a sunrise or a sunset in the satellite’s frame of reference) to 6 km for occultations in which the sun rises (or sets) perpendicular to the Earth horizon. Vertical sampling depends on the absolute value of the angle between the orbit track of the satellite and the Earth-Sun vector – the so-called beta angle. The greater the value of beta, the smaller the distance between vertical samples. During a single year vertical sampling completes six cycles of going from high vertical sampling (<2 km altitude) to low sampling (<6 km altitude) and back to high sampling again. The highest vertical sampling (<2 km) occurs in the months of February, April, June, August, October and December, with the lowest sampling in the other six months.

Temperatures and pressures are interpolated to a 1 km vertical grid assuming the atmosphere is in hydrostatic equilibrium (Boone et al., 2005) to match the higher resolution of a second instrument on board the satellite called MAESTRO (Measurement of Aerosol Extinction in the Stratosphere and Troposphere Retrieved by Occultation). One of the level 2 data products of the satellite is the temperature profile specified at 1 km intervals in the altitude range 0.5 to 149.5 km for each occultation event. The temperature profiles produced by Version 2.2 of the ACE-FTS processing software were used in this study. Typically there are approximately 15 orbits per day each containing one sunrise and one sunset event. The time of measurement and geographic coordinates of each occultation event are known with a high degree of accuracy. Over the course of the period of the data considered (January 2004–December 2005), more than 8000 temperature profile

measurements have been made available. Figure 2 is a typical temperature profile selected here because its latitude and longitude coordinates (54.44° N, 4.13° W) are close to the observing station at Maynooth. Uncertainties of 3–5 K are quoted for the temperature retrievals (Boone et al., 2005) which include statistical fitting errors assuming a normal distribution of random errors, but do not take account of systematic contributions. Recently published validation work using both ground-based and space-borne measurements (Sica et al., 2007) shows ACE-FTS temperatures to be in agreement with other sensors to better than ~5 K in the lower mesosphere.

Although designed primarily as a stratospheric experiment, the ACE-FTS temperature data represents a potentially very valuable resource for atmospheric study outside of the principal region of interest. The very extensive latitude coverage over all longitudes and local times between 80° S and 80° N offers the potential for ACE-FTS to act as a transfer standard for comparing temperatures measured at different locations and by different techniques over almost the entire Earth. In the present study, the temperatures of interest are those in the vicinity of the mesopause. The OH Meinel bands in the near-infrared have long been used (see e.g. Sivjee, 1992) to determine mesopause temperature because they are among the brightest airglow features in the night sky. We have determined an OH-equivalent temperature (described in detail in Sect. 3) from each satellite temperature profile. Averages of these temperatures over a period of two years were then compared with ground-based measurements over a similar period. It was intended initially to perform a comparison of ACE-FTS OH equivalent temperatures only with Maynooth ground-based data. However, as will become clear

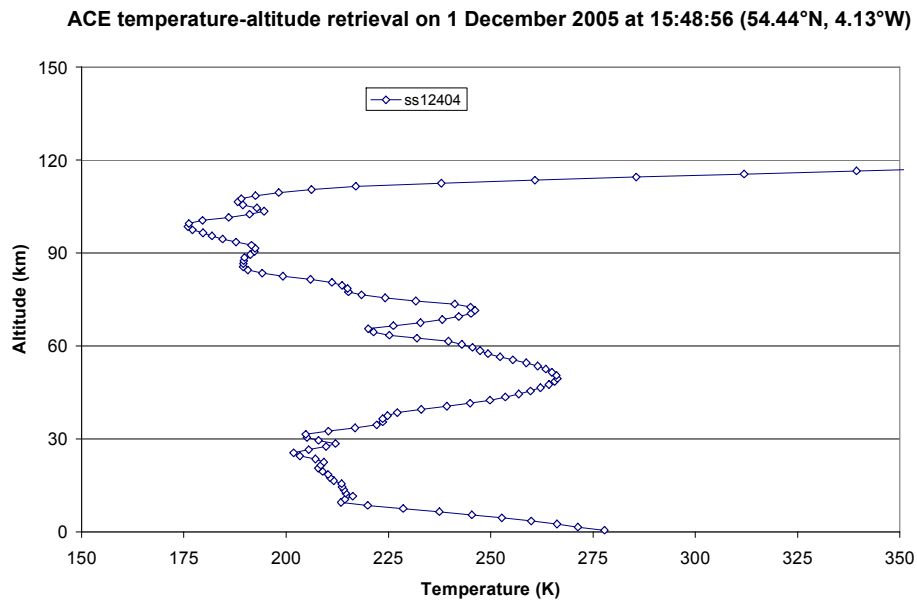


**Fig. 2.** A typical ACE-FTS temperature-altitude profile from the sunset occultation of orbit 12404 on 1 December 2005 at 15:48:56 (54.44° N, 4.13° W).

later in this report, knowledge of the behaviour of the OH layer is vital for this comparison. ACE-FTS does not measure the OH volume emission ratio (VER) profile. SABER data was included in the comparison because SABER provides a simultaneous measurement of both the temperature and OH VER profile.

### 2.3 SABER data

The SABER (Sounding of the Atmosphere by Broadband Emission of Radiation) instrument on board NASA's Thermosphere Ionosphere Mesosphere Energetics and Dynamics (TIMED) satellite was designed to measure temperature and chemical species in the MLT region of the atmosphere. It was launched in December 2001 into a 625 km orbit inclined at 74 degrees to the equator. SABER measures vertical Earth limb emission profiles in the wavelength range 1.27  $\mu\text{m}$  to 17  $\mu\text{m}$ . Kinetic temperatures are determined from 15  $\mu\text{m}$  CO<sub>2</sub> emissions, taking account of the non-LTE conditions in the MLT region, in combination with 4.3  $\mu\text{m}$  CO<sub>2</sub> emission used to derive the CO<sub>2</sub> volume mixing ratio (Mertens et al., 2004). The TIMED satellite orbits the Earth about 15 times per day, and measures approximately 100 vertical profiles in each orbit. SABER has a vertical resolution of about 2 km in the altitude range 10–105 km, and an along track resolution of approximately 400 km. SABER temperatures from data version 1.06 were used in this work. Preliminary estimates of temperature error are quoted as 5 K for the systematic error and 2 K for the precision at 87 km.

## 3 Methodology and data analysis

### 3.1 Validation of Maynooth airglow data

We begin this section by comparing OH\*(3-1) temperatures obtained at Maynooth in 1994 with results obtained from the same band in that year at two ground-stations – Wuppertal (51.3° N, 7.2° E) (Offermann et al., 2006) and Stockholm (59.5° N, 18.2° E) (Espy and Stegman, 2002) – that have latitudes similar to Maynooth. An averaged nightly temperature was calculated for each night on which temperature data was recorded at all three ground stations. For the Maynooth data, the contribution of each temperature to the nightly average is weighted according to the inverse-square its individual measurement uncertainty (Bevington, 1992). Each nightly averaged temperature for the two-year period, 1993–1994, was then binned according to the day of the year into 30-day windows centred at 15-day intervals. An average temperature was calculated at the centre of each window. The overlap of the windows meant that the final 15 days of window  $n$  was also included as the first 15 days of day  $n+1$ . The Wuppertal and Stockholm data were processed in the exactly same manner as the Maynooth data and all three data sets are plotted in Fig. 3 for the year 1994. As expected, the highest latitude station (Stockholm) has the lowest summer temperatures. The summer temperatures recorded at Maynooth lie between those obtained at Wuppertal and Stockholm, which is consistent with its intermediate latitude between these two stations. The Maynooth winter temperatures are slightly higher in spring than either Wuppertal or Stockholm and are almost identical to the Stockholm values in winter.

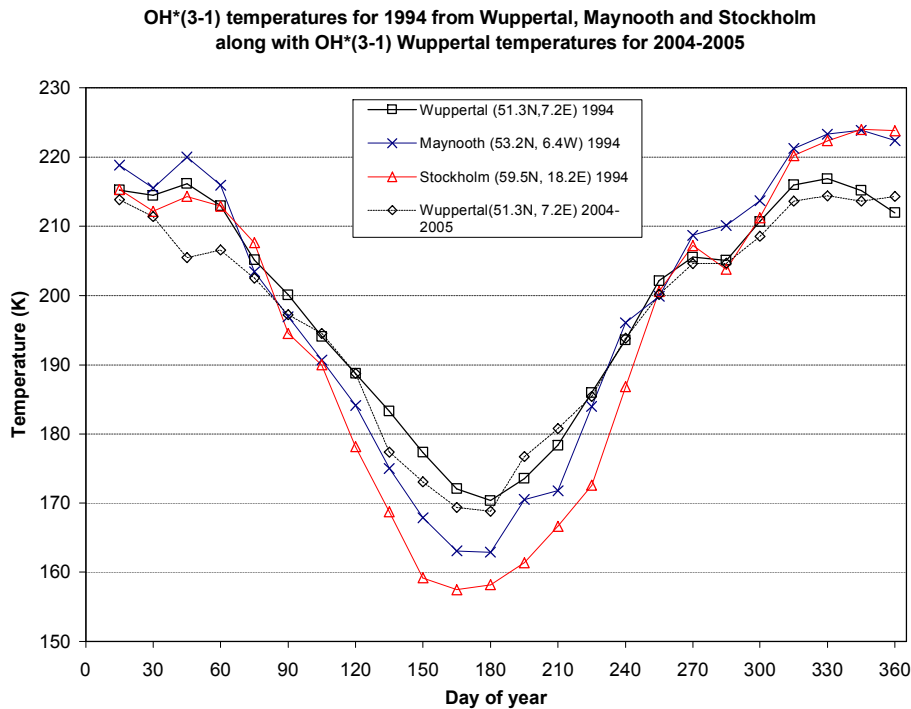


**Fig. 3.** A comparison of OH\*(3,1) rotational temperatures recorded at 3 ground-based stations, Stockholm (59.5° N, 18.2° E), Maynooth (53.2° N, 6.4° W) and Wuppertal (51.3° N, 7.2° E) for 1994. Also shown for comparison purposes are monthly averaged temperatures for Wuppertal for 2004–2005.

The combination of data from the three stations suggests that the values reported for Maynooth are representative of other ground-based OH\*(3-1) temperatures. As a further check on the validity of the ground-based data, Fig. 3 also shows 30-day averaged monthly temperatures for Wuppertal during the period 2004–2005 which supports the assumption that the annual cycle in the mesopause temperature has remained essentially constant over the past decade.

### 3.2 Calculation of OH-equivalent temperatures from satellite temperature profiles

Following the work of Baker and Stair (1988), the mean altitude profile of the Meinel hydroxyl emission band is usually considered to have a maximum near 87 km altitude and to have a full width at half maximum (FWHM) intensity of 8–10 km. These values have been confirmed by the results of She and Lowe (1998), and Oberheide et al. (2006) among others. Indeed, the degree of consistency reported for the height of this layer was one of the factors that prompted the type of statistical comparison undertaken here. As a result of measurements by the WINDII instrument on the UARS satellite (Lowe, 1995; Zhang and Shepherd, 1999; Liu and Shepherd, 2006), it is now known that the altitude of the peak emission of the OH\*(3-1) Meinel band undergoes small departures ( $< \pm 3$  km) as a function of time of year, latitude and phase of the solar cycle. We return to this point in detail in

the discussion, but for the moment we treat the OH emission as if it arises from a globally uniform stable layer fixed in altitude and in depth.

The temperatures available from the ACE-FTS instrument are specified at a vertical spacing of 1 km in the range 0.5–149.5 km in altitude, while SABER temperatures are specified with a vertical spacing of 0.4 km. Ground based temperatures represent a type of weighted average temperature over the height of the emitting layer. The weighting function is in essence the altitude profile of the OH emission itself. In order to facilitate a comparison of the satellite temperature profiles with the ground-based data, it is necessary to calculate an equivalent OH temperature from each temperature profile. von Zahn et al. (1987) were the first to apply the concept of an OH-equivalent temperature when comparing ground-based OH\*(3-1) temperatures with temperature profiles obtained by lidar. The method was used subsequently by She and Lowe (1998) who distinguished between a brightness weighted temperature,  $T_B$ , in which the temperature profile is combined with the volume emission rate profile, and the more exact OH-equivalent temperature,  $T_{rot}$ , (representing the rotational temperature) in which the temperature profile in combination with the VER profile is used to calculate a vertically-integrated intensity  $I_{J'}$  for each of the three hydroxyl emission lines ( $P_1(2)$ ,  $P_1(3)$  and  $P_1(4)$ ) in the spectra that are used to determine the temperature from the Fourier transform spectrometer. The brightness weighted

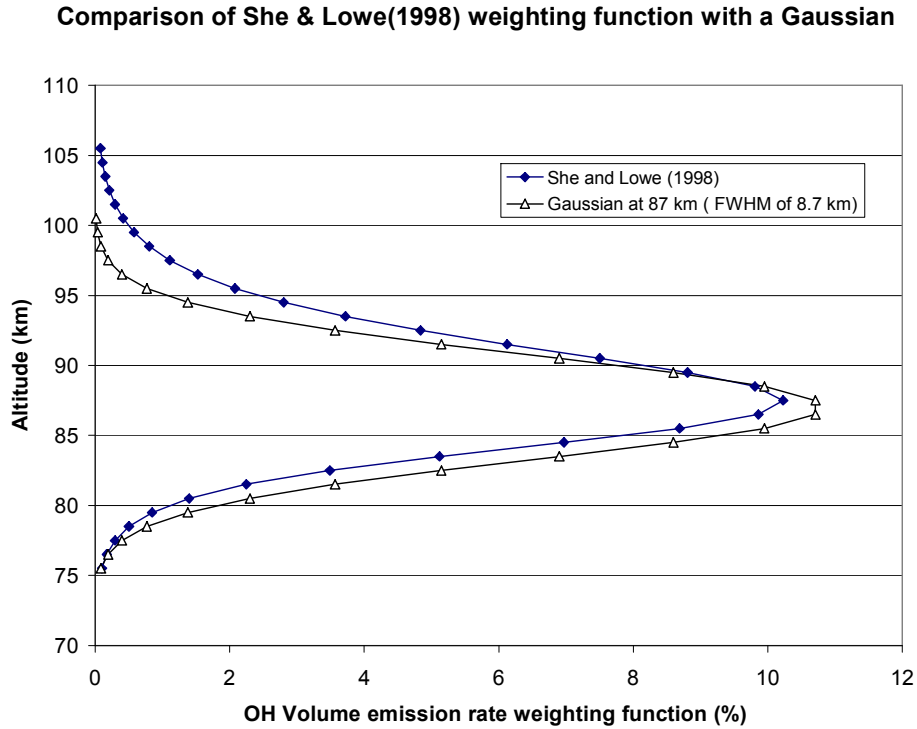


**Fig. 4.** A comparison of the Gaussian weighting function (centred on an altitude of 87 km with a full width at half maximum of 8.7 km) with the volume emission rate profile from She and Lowe (1998). The latter was used as the weighting function in deriving the OH-equivalent temperatures reported here.

temperature is calculated as

$$T_B = \left( \sum_z T(z) \cdot \text{VER}(z) \right) / \left( \sum_z \text{VER}(z) \right)$$

where  $z$  is the altitude,  $T(z)$  is the temperature profile and  $\text{VER}(z)$  is the OH volume emission rate profile.  $T_{\text{rot}}$  is obtained from the intensities of the three most intense lines in the OH\*(3-1) band in exactly the same fashion as in the case of the spectrometer, where each intensity is calculated as:

$$I_{J'} = \sum_z \text{VER}(z) \cdot A_{J'} \cdot 2(2J' + 1) \cdot e^{(-E(J')/kT(z))}$$

where  $J'$  is the rotational quantum number corresponding to each of the three emission lines,  $A_{J'}$  is the transition probability for each line,  $E(J')$  is the energy of one photon at the line in question, and  $k$  is the Boltzmann constant.  $T_{\text{rot}}$  is calculated as the negative inverse of the slope of a plot of  $\ln\{I_{J'}/(A_{J'} \cdot 2(2J'+1))\}$  versus  $E(J')$ . Makhlouf et al. (1995) have reported the effect of using either  $T_B$  or  $T_{\text{rot}}$  in a photochemical-dynamical model of the measured response of airglow to gravity waves. She and Lowe (1998) pointed out that the brightness temperature method is susceptible to the small non-linear variation of intensity with temperature, which can give rise to a temperature difference of a few degrees if the temperature profile contains steep

gradients of the order of 10 K/km. While one of the characteristics of the mesopause is a slowly changing temperature as a function of altitude, it should be noted that gradients in excess of 40 K/km near 90 km have been observed by Fritts et al. (2004) in summer mesopause conditions. Both von Zahn et al. (1987) and She and Lowe (1998) used the more exact method in preference to the brightness temperature. More recently, Oberheide et al. (2006), and López-González et al. (2007) have used the brightness temperature method when converting SABER temperature profiles from the TIMED satellite into OH-equivalent temperatures using the OH emission profile determined Baker and Stair (1988), i.e. a Gaussian shaped weighting function centred at 87 km with a full-width at half maximum of 8.7 km. In the reports of von Zahn et al. (1987), She and Lowe (1998), Oberheide et al. (2006) and López-González et al. (2007), as in the present work, differences in the field-of-view of the techniques being compared can contribute to differences in the temperatures. However, it is expected that the extent of the averaging employed should effectively eliminate any significant trend.

### 3.3 ACE-Maynooth comparison

In the ideal case we would have simultaneous temperature and OH VER profiles from which to compute the OH equivalent temperature. Since ACE does not measure the OH VER,

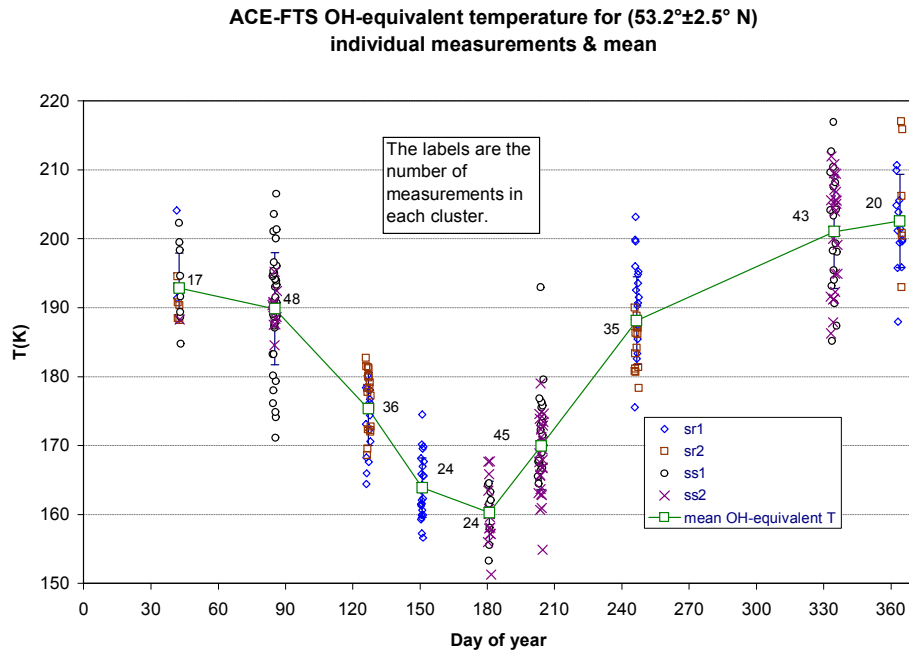


**Fig. 5.** OH-equivalent temperatures for all of the ACE-FTS profiles (292) within a  $\pm 2.5$  degree band of latitude centred on the observing station at Maynooth ( $53.2^\circ \text{ N}$ ,  $6.4^\circ \text{ W}$ ). The orbit of the satellite causes the measurements to cluster around certain days of the year (sr/ss refer to a sunrise/sunset occultation; sr1 refers to orbits 1–10 000, while sr2 refer to orbit numbers > 10 000). The average temperature for each of the clusters is also plotted and it is assigned to the day in the centre of the cluster.

we adopted a statistical approach and used a globally averaged OH VER profile.

We initially calculated OH-equivalent temperatures using the brightness weighted temperature method. The weighting function used was based on the OH volume emission rate profile determined by She and Lowe (1998), since the number of profiles on which it is based is far greater than that used in the original determination by Baker and Stair in 1988. We subsequently calculated OH-equivalent temperatures using the more precise method employed by both von-Zahn et al. (1987) and She and Lowe (1998), but found that the temperatures obtained differed by an average of only  $0.22 \pm 0.14 \text{ K}$ , with  $T_B$  always higher than  $T_{rot}$ . The maximum difference obtained between the two methods of temperature calculation was 0.9 K. Figure 4 shows a comparison of the Gaussian weighting function with the She and Lowe (1998) profile used in this work. The latter has a less dramatic fall off at the high altitude side with the result that its centroid is approximately 1 km higher in altitude than the Gaussian with a peak at 87 km.

The She and Lowe weighting was applied to each ACE-FTS temperature profile that fell within  $\pm 2.5$  degrees latitude of the Maynooth station regardless of longitude in order to calculate an equivalent OH temperature. Figure 5 shows all of the temperature values thus obtained for the 292 ACE-FTS profiles that satisfied the latitude criterion. Because of the orbit of the satellite, measurements tend to cluster around

certain days of the year. All longitudes and times are equally represented within the 5 degree latitude band, and no significant difference was found between the temperatures determined from profiles retrieved from sunset and sunrise. All of the OH-equivalent temperatures in a given cluster were then averaged and the average was assigned to the day of the year in the centre of the cluster as shown in Fig. 5. The value so assigned is the average over a broad range of longitudes, (i.e. each point is a zonal average); hence any variation that might be present due to planetary scale waves would be expected to be averaged out in the daily averaged ACE-FTS data, just as it would be expected to be averaged out in the 30-day averaged ground-based data described in Sect. 3.1.

In order to understand the effect of calculating an OH-equivalent temperature for the ACE-FTS data, we calculated the average temperature at a fixed height of 87 km for the clusters in Fig. 5, together with OH-equivalent temperatures using the Gaussian weighting function. Figure 6 shows all three temperature values for each of the clusters shown in Fig. 5. The average of the OH-equivalent temperatures determined using the two different weighting functions is almost identical (182 K). However, the OH-equivalent temperatures obtained using the She and Lowe weighting are approximately 2 K higher in summer and between 2 and 3 K lower in winter than the corresponding temperatures obtained using the Gaussian weighting as illustrated in Fig. 6.

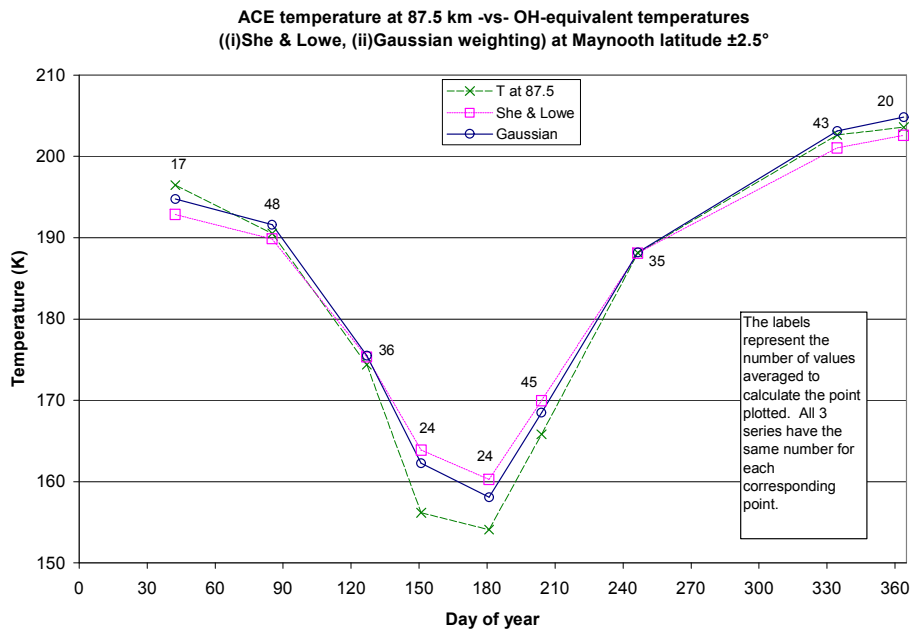


**Fig. 6.** A comparison of the temperature at 87.5 km averaged over all of the profiles that comprise each cluster in Fig. 5 with the averaged OH-equivalent temperature calculated using (i) the She and Lowe (1998) volume emission rate weighting function, and (ii) the Gaussian weighting function centred on 87 km with a full width at half maximum of 8.7 km.

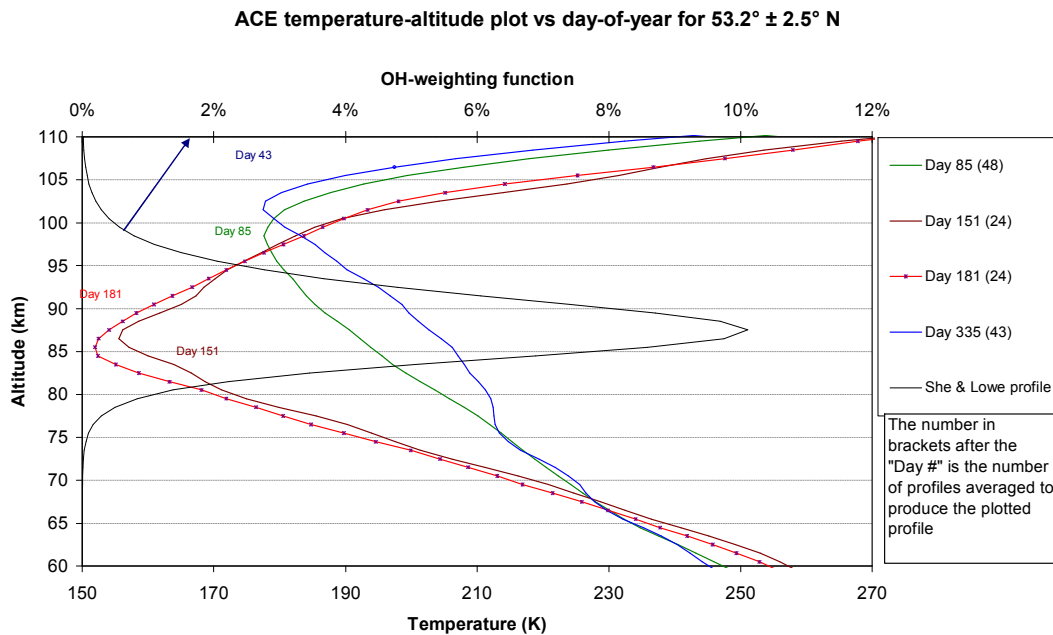


**Fig. 7.** The average temperature profile for two summer days (day 151 and 181) and two winter days (day 43 and day 85) shown in Fig. 5 are illustrated by reference to the day of the year of each cluster. Also shown is the She and Lowe (1998) weighting function for illustrative purposes. The lower x-axis applies to the temperature profiles, while the upper x-axis refers to the weighting functions.

Figure 6 also shows that the OH-equivalent temperature (regardless of the weighting function used) is higher in summer than the average temperature at 87 km by approximately 6 K, and that the situation is reversed in winter but with the

difference less than  $\sim 2$  K. This effect can be understood by examining the average temperature profile as a function of day of the year, illustrated in Fig. 7, for the clusters shown in Fig. 5. During the winter, the temperature at 87 km is a very



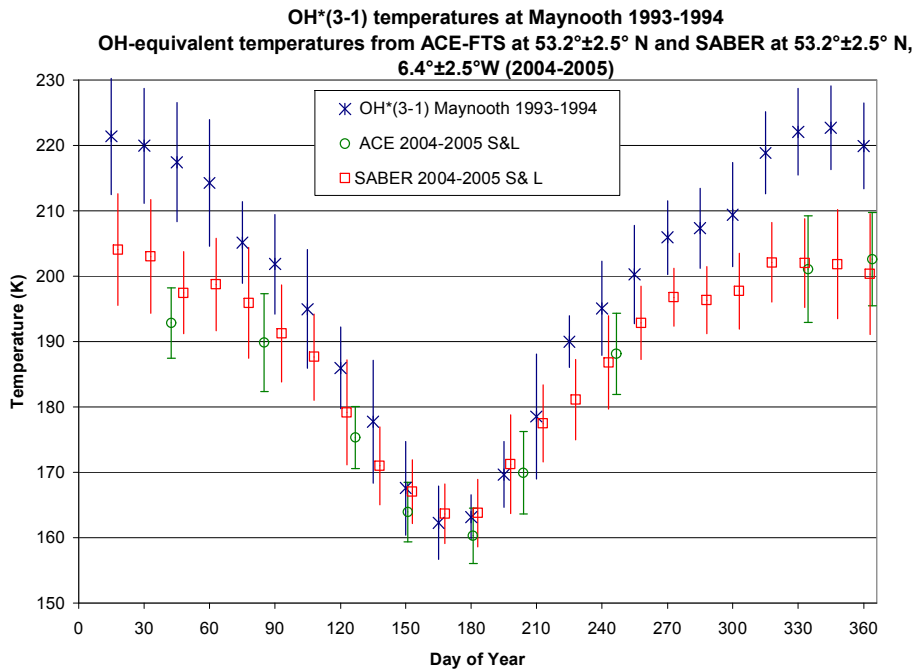


**Fig. 8.** ACE-FTS OH-equivalent temperatures for a zonally averaged 5 degree latitude band centred on Maynooth compared with the OH\*(3-1) 30-day moving average rotational temperature (at 15-day intervals) recorded at Maynooth in 1993 and 1994. Also shown in this figure for comparison purposes are 30-day averaged OH-equivalent temperatures for 2004 and 2005 from the SABER instrument (calculated in the same way as the ACE-FTS temperatures) on the TIMED satellite at  $53.2^{\circ} \pm 2.5^{\circ}$  N,  $6.4^{\circ} \pm 2.5^{\circ}$  W. The SABER points have been offset by +2 days on the x-axis to improve the clarity of the figure. The error bars are one standard deviation in all cases.

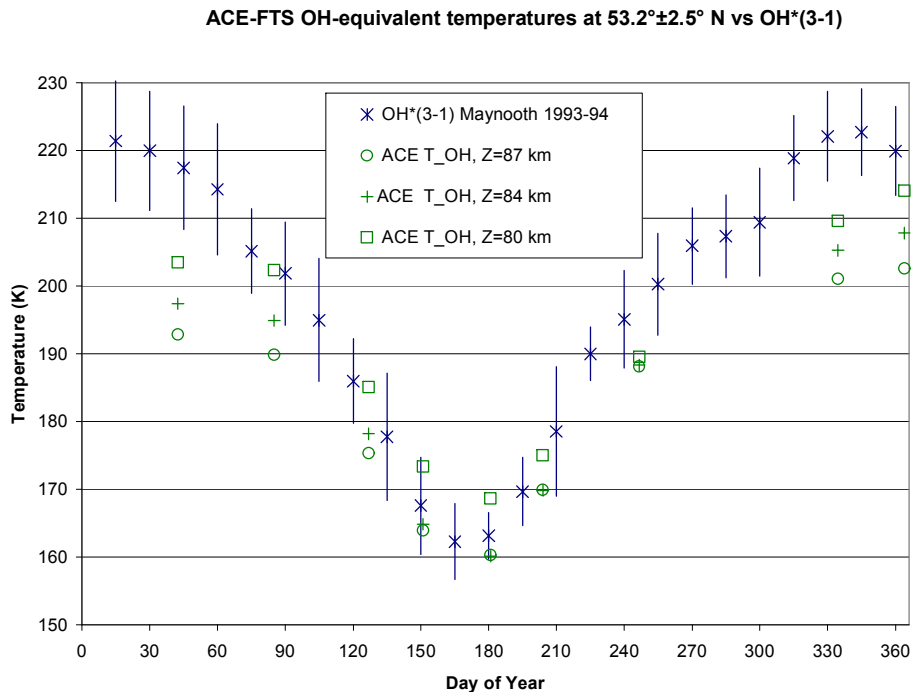
good estimate for the OH-equivalent temperature determined by the weighting function (also shown in Fig. 7) because the average temperature profile tends to be approximately linear along the most influential part of the weighting function. In the summer however, the temperature profile shows a pronounced minimum near 87 km with the result that the weighting function tends to increase the OH-equivalent temperature. Figure 7 also provides very convincing evidence of the existence of the two-level mesopause (high in winter near 100 km and low in summer near 86 km) first reported by von Zahn et al. (1996).

Figure 8 shows both the ground-based 30-day averaged temperatures together with the mean OH-equivalent ACE-FTS temperatures. The error bars associated with the points plotted are  $\pm 1$  standard deviation ( $\sigma$ ) in the data and they are primarily the result of geophysical variations rather than an inherent uncertainty in the measurements. Since the processing of ACE-FTS data has not yet reached the point of including systematic contributions in the uncertainties reported for the temperatures in an altitude profile, we simply note that the precision of the averaged values determined here is comparable to the ( $< 1$  K) precision of the ground-based averaged temperatures.

The ground-based and satellite data in Fig. 8 exhibit an annual cycle with a cold summer and warmer winter mesopause. They also show excellent agreement in the low

temperatures reached near summer solstice ( $\sim 162$  K). Away from summer solstice, however, the ground based temperatures begin to show higher values than the ACE-FTS OH-equivalent, with the maximum difference occurring in winter. A maximum disagreement of up to 20 K is observed in mid-winter. This degree of divergence between the datasets is surprising, being far greater than the degree of precision associated with either set, and it suggests that either the ground-based or the ACE-FTS data set (or both) may include a systematic offset. It is known that some of the emission lines in the OH\*(3-1) vibration-rotation band undergo absorption by water vapour in the lower atmosphere (Turnbull and Lowe, 1983). The increased water vapour content in summer has the potential to introduce a seasonal bias in the ground-based temperatures. However, the  $P_1(2)$ ,  $P_1(3)$  and  $P_1(4)$  lines in the OH\*(3-1) band were selected for temperature determination specifically because they are not affected to any significant extent by water vapour absorption.

All of the OH\*(3-1) temperatures were obtained during the night, whereas the ACE-FTS temperatures were sampled uniformly throughout the 24 h period. A large diurnal tide with a seasonal variation could produce the type of temperature difference illustrated in Fig. 8. As was mentioned in Sect. 2.1, the Maynooth ground-based data are biased to have a greater number of measurements per night in the winter. The shorter observing period in the mid-summer could give



**Fig. 9.** A comparison of OH-equivalent temperatures calculated for different peak altitudes (80 km, 84 km and 87 km) of the She and Lowe (1998) weighting function together with the OH\*(3-1) temperatures from Maynooth. The error bars on the Maynooth data are one standard deviation.

rise to a bias arising from non-cancellation of either the diurnal or semidiurnal tide. The magnitude of either tide is not expected to be large at these latitudes (Zhang and Shepherd, 1999). Nevertheless, we examined the ACE-FTS temperatures for tidal variations but found no evidence to support this possibility. We repeated the examination for a wider band of latitude ( $\pm 7.5$  degrees) centred on the Maynooth station in order to improve the statistics, but we were still unable to find evidence of any significant tidal variation that might explain the temperature difference shown in Fig. 8.

The disagreement between the OH-equivalent temperatures and the ground-based measurements in winter time can easily be attributed to the fact that a constant altitude profile was used in calculating the OH-equivalent temperatures, whereas in reality, the OH emission layer changes its altitude as a function of season and latitude (Lowe, 1995; Zhang and Shepherd, 1999; Liu and Shepherd, 2006). In addition, the profile of the OH VER departs from a simple layer to a more complex structure between 5 and 25% of the time (Melo et al., 2000), with a two-peaked structure being the most common. In the following paragraph, we attempt to take account of the altitude change.

Liu and Shepherd (2006) developed an empirical model for the altitude of the OH nightglow emission based on VER profiles of the OH(8-3)  $P_1(3)$  line at 743 nm. Unfortunately we were unable to use the model because its coverage is limited to the latitude region  $40^{\circ}$  S to  $40^{\circ}$  N; it also requires

knowledge of the integrated emission rate, which is not measured by ACE-FTS. The orbit of UARS was such that the majority of the WINDII data in the latitude range  $50^{\circ}$ – $60^{\circ}$  N was confined to the 6 months centred on the winter solstice. The altitude of the peak emission of OH determined from these orbits was in the range 84–88 km with the lowest altitudes tending to occur at winter solstice (Lowe, 1995). Figure 7 shows that if the weighting function were centred on a lower altitude, the resulting OH-equivalent temperature would be increased in winter time, thereby reducing the temperature difference between the satellite and ground based measurements. We computed the OH-equivalent temperature using the She and Lowe weighting function centred on a range of altitudes. The temperature difference between the two data sets in winter was reduced to approximately 14 to 15 K by lowering the peak altitude of the weighting function to 84 km. However, we found that the peak altitude had to be placed unrealistically low to obtain agreement between the satellite and ground-based data in winter. Figure 9 shows the effect of lowering the peak altitude of the weighting function on the computed OH-equivalent temperatures from ACE-FTS, together with OH\*(3-1) temperatures from Maynooth. The OH-equivalent temperatures at summer solstice are relatively insensitive to small changes ( $< 3$  km) in the peak altitude of the weighting function, in contrast to the winter values which show maximum sensitivity in this regard.

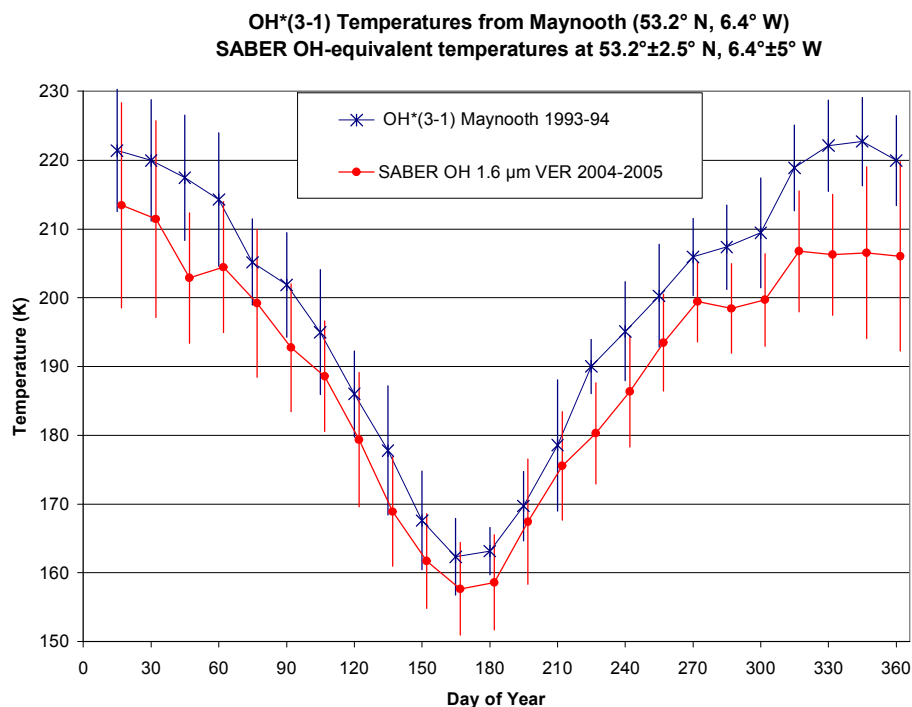


**Fig. 10.** OH\*(3-1) rotational temperatures recorded at Maynooth in 1993 and 1994 together with OH-equivalent temperatures calculated from SABER temperature profiles at Maynooth in 2004 and 2005 using the SABER OH 1.6  $\mu\text{m}$  VER profile as the weighting function. The SABER points have been offset by +2 days on the x-axis to improve the clarity of the figure. The error bars are one standard deviation in all cases.

In summary, we were unable to find a satisfactory explanation for the discrepancy in the 30-day averaged winter values. We decided to examine data from a second satellite as a check on the ACE-FTS data. SABER/TIMED was chosen because it has temperature profiles that were obtained in the time period under study, and has the added advantage that it makes measurements of the OH VER profile.

### 3.4 SABER-Maynooth comparison

SABER measures the OH VER profile in the range 1.56–1.72  $\mu\text{m}$  which includes mostly the OH\*(4-2) and OH\*(5-3) bands. We discuss in detail the effect of using this profile to calculate the OH equivalent temperature at the end of this section, but at this point we use the same globally averaged OH VER profile to calculate OH equivalent temperatures in order to treat the data from both satellites in a consistent way. The temperatures available from the SABER instrument are specified at a vertical spacing of 0.4 km in the range 12 km–140 km in altitude. SABER measures approximately 100 profiles for every two measured by ACE-FTS. As a result, it was not necessary to employ the zonal averaging used in the case of the ACE-FTS data. OH equivalent temperatures were calculated (in the same way as the ACE-FTS temperatures) from each SABER temperature profile that was obtained within  $\pm 2.5^\circ$  latitude and  $\pm 5^\circ$  longitude of

the station at Maynooth for the same time period as the ACE-FTS data. The number of profiles that satisfied these selection criteria for the 2004–2005 time period was 1018. Each SABER point shown in Fig. 8 is a 30-day average of the OH-equivalent temperatures, and error bars are  $\pm 1\sigma$ . The agreement between the two satellite datasets is very good apart from days 43 and 87, at which the ACE-FTS values are 4–7 K lower. ACE-FTS is also a few K lower in mid-summer. Validation work on ACE-FTS temperature profiles (McHugh et al., 2005; Sica et al., 2007; Schwartz et al., 2008) indicates that in general they are in good agreement with temperature profiles from other satellites. Up to 10% of ACE-FTS temperature profiles are affected by unphysical oscillations as large as 10 K in the mesosphere in version 2.2 of the retrieval software. The cause of this problem has been identified and it will be resolved in the next generation of the ACE-FTS software (Sica et al., 2007). Profiles that exhibited these unphysical oscillations were excluded from the calculation of OH-equivalent temperatures reported here. The comparison of the two satellite datasets in Fig. 8 is a test of the zonal averaging employed in the case of the ACE-FTS data (because of the paucity of profiles) and indicates that the method provides a good representation of the temperature at the latitude under consideration.

In an ideal scenario, we would have simultaneous measurements of temperature and volume emission rate profiles

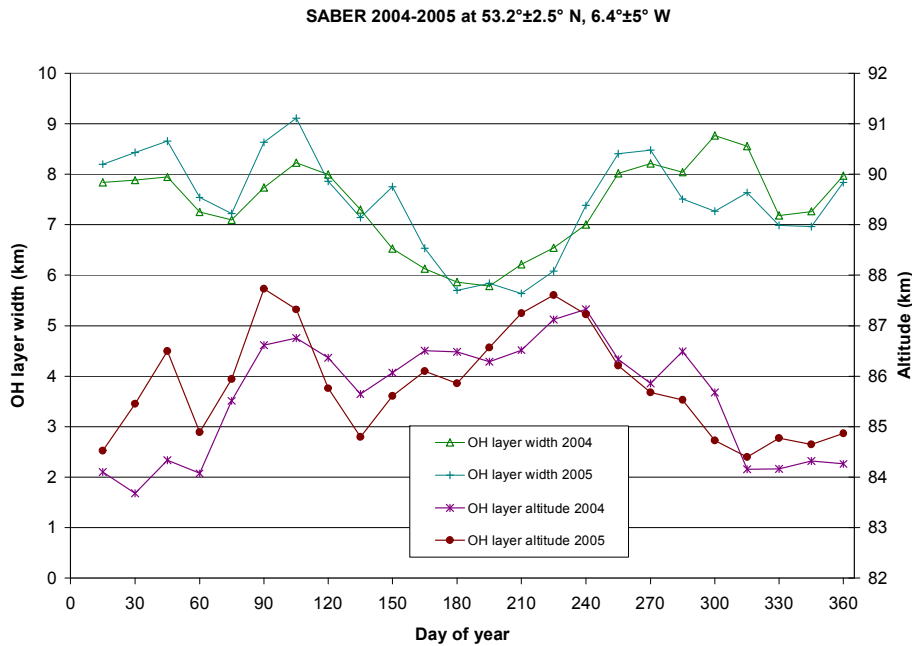


**Fig. 11.** Altitude of the maximum intensity and full width at half intensity of the SABER OH  $1.6\ \mu\text{m}$  VER profile during 2004 and 2005 at Maynooth plotted as 30-day averages.

of the OH\*(3-1) band. This would enable us to compute OH-equivalent temperatures using the appropriate weighting function. SABER measures the OH VER profile in the range  $1.56\text{--}1.72\ \mu\text{m}$  which includes mostly the OH\*(4-2) and OH\*(5-3) bands. Oberheide et al. (2006) reported that the goodness of fit between satellite OH equivalent temperatures and their ground based data deviated from unity when they employed the OH  $1.6\ \mu\text{m}$  VER profile as the weighting function. They speculated that the result might have been because the measured  $1.6\ \mu\text{m}$  VER profile is not a true representation of the OH\*(3-1) band. However, altitude differences between the lowest and highest vibrational OH levels are not expected to exceed 2 km (McDade, 1991). On the basis that the SABER OH  $1.6\ \mu\text{m}$  VER was the best available measure of the OH profile, we calculated an OH equivalent temperature for each SABER profile using its corresponding OH  $1.6\ \mu\text{m}$  VER. The resulting plot is shown in Fig. 10. The OH-equivalent winter temperatures increased as expected, but this was accompanied by a decrease in the summer OH-equivalent temperatures. A detailed examination of the SABER OH  $1.6\ \mu\text{m}$  VER showed that both the height of the layer and its thickness are highly variable even on time scales as short as one day. A thinner OH layer in summer gives rise to a reduced OH-equivalent temperature as is clear from the averaged profiles for ACE-FTS shown in Fig. 7. Figure 11 shows the 30 day averaged peak altitude and width at half-intensity of all the OH  $1.6\ \mu\text{m}$  VER profiles for 2004 and 2005. While an overall seasonal trend is discernable in both the altitude and the half-width of the OH

layer, we found that correcting 30-day averaged temperature profiles for SABER using the 30-day averaged altitudes and widths shown in Fig. 11 did not reproduce exactly the 30-day averaged temperatures obtained when each temperature profile was weighted by its corresponding the OH  $1.6\ \mu\text{m}$  VER profile. Differences as large as 7–8 K were obtained in some cases. We attribute this to the timescale of variability of the OH layer. We believe it is an important result for those attempting to reconcile temperatures measured by ground-based instruments with equivalent temperatures derived from satellite temperature profiles. Since we were unable to correct the SABER 30-day averaged temperature profiles for the altitude and width of the layer, we considered attempting to correct the ACE-FTS averaged temperature profile a futile exercise.

Figure 10 shows that after applying the OH  $1.6\ \mu\text{m}$  VER to its own temperature profile, the OH-equivalent temperatures now have an overall cold bias with respect to the ground based OH\*(3-1) temperatures. A least squares linear fit of the ground-based and SABER data taking account of the uncertainty in both datasets (Reed, 1992 and references therein) gives a slope of  $1.15\pm 0.03$ , which indicates that the average offset ( $8.6\pm 0.8\ \text{K}$ ) is temperature dependent. Bearing in mind that the satellite and ground based data are separated by more than a decade, the value of the offset obtained is comparable to the  $7.5\pm 0.5\ \text{K}$  value obtained by Oberheide et al. (2006) for nearly coincident data.

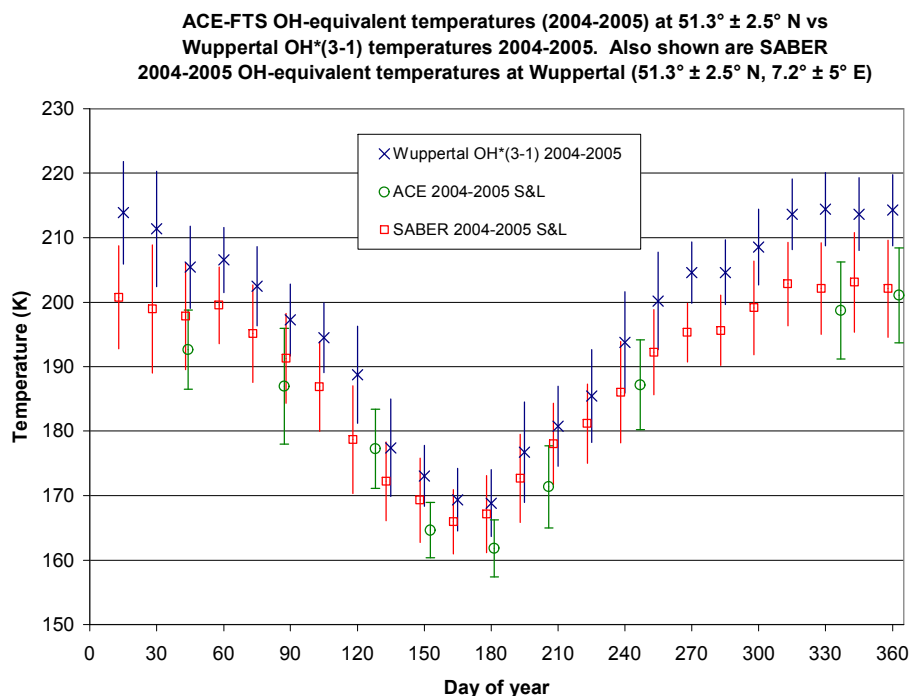


**Fig. 12.** ACE-FTS OH-equivalent temperatures for a 5 degree latitude band centred on Wuppertal compared with the OH\*(3-1) 30-day moving average rotational temperature (at 15-day intervals) recorded at Wuppertal in 2004 and 2005. Also shown in this figure are 30-day averaged OH-equivalent temperatures for 2004 and 2005 from the SABER instrument (calculated in the same way as the ACE-FTS temperatures) on the TIMED satellite at  $51.3^{\circ} \pm 2.5^{\circ}$  N,  $7.2^{\circ} \pm 5^{\circ}$  E. The SABER points have been offset by  $-2$  days on the x-axis to improve the clarity of the figure. The error bars are one standard deviation in all cases.

#### 4 Discussion

It might be argued that the cold temperature bias found here arises from the fact that the ground-based data is separated in time by more than a decade from the two satellite datasets, and that the solar cycle may influence the average temperatures obtained. The comparison attempted here is based on the premise that the mean annual temperature cycle at mesopause altitudes has altered very little over the past decade. Several authors have attempted to detect a change in the temperature of the mesopause over periods greater than one solar cycle, e.g. Bittner et al. (2000), Sigernes et al. (2003). These reports have been summarised by Beig et al. (2003) who conclude that current results are inconclusive on the presence of any long term trend in the temperature at the mesopause. A recent simulation study of secular trends in the middle atmosphere over the period 1950–2003 by Garcia et al. (2007) shows that any trend in the vicinity of the mesopause is less than 0.5 K/decade. Marsh et al. (2006) found that the solar cycle effect due to radiative and geomagnetic forcing was in the range 2–5 K at altitudes in the 80–100 km region. The effect on the temperatures obtained in this study is expected to be very low due to the fact that the difference in time between the two data sets is almost exactly one solar cycle.

Despite the attempts to find an explanation for the temperature difference obtained above, the lack of coincidence between the ground-based data and the two satellite datasets represents a weakness in the comparison. Since ground-based data for Maynooth corresponding to the satellite measurement period is not available, this difficulty cannot be overcome completely. Instead, OH\*(3-1) temperatures from the Ground-based Infrared P-branch Spectrometer (GRIPS) data at Wuppertal ( $51.3^{\circ}$  N,  $7.2^{\circ}$  E) (Offermann et al., 2006) that are coincident with the satellite measurement period under consideration have been used as a proxy for the Maynooth station. The comparison described above for the Maynooth data was repeated for the Wuppertal data in the case of both ACE-FTS and SABER temperature profiles. Figure 12 shows a comparison of Wuppertal OH\*(3-1) temperatures for the years 2004 and 2005 with OH equivalent temperatures for the same period derived from both ACE-FTS and SABER using the She and Lowe weighting function. The temperatures derived from the satellites are in good agreement, but they are both colder than the OH\*(3-1) temperatures in winter although the offset is not as pronounced as in the case of the Maynooth data from eleven years earlier. Figure 13 shows the effect of applying to each SABER temperature profile its corresponding OH  $1.6 \mu\text{m}$  VER as the weighting function. As in the case of the SABER data at

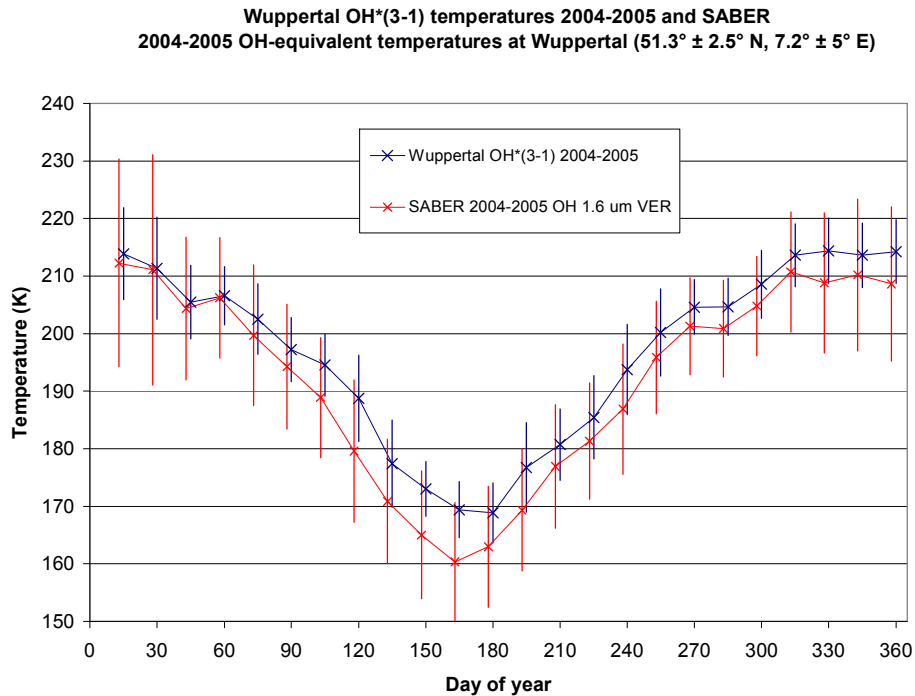


**Fig. 13.** OH\*(3-1) rotational temperatures from Wuppertal in 2004 and 2005 together with OH-equivalent temperatures calculated from SABER temperature profiles at Wuppertal in 2004 and 2005 using the SABER OH  $1.6\ \mu\text{m}$  VER profile as the weighting function. The SABER points have been offset by  $-2$  days on the x-axis to improve the clarity of the figure. The error bars are one standard deviation in all cases.

Maynooth, the OH equivalent temperatures increased in winter and decreased in summer. The slope of the best fit line to the two data sets shown in Fig. 13 taking account of the error in both parameters was found to be  $0.9 \pm 0.02$  and the offset was found to be  $4.5 \pm 0.5$  K

López-González et al. (2007) recently reported SABER (version 1.06) temperatures to have a cold bias of  $6.8 \pm 9$  K at 87 km compared with temperatures from the Spectral Airglow Temperature Imager (SATI) instrument at Sierra Nevada Observatory ( $37.06^\circ$  N,  $3.38^\circ$  W). The bias was reduced to 5.7 K when weighted with a typical OH emission layer of 10 km half width centred on 87 km. A comparison of ACE-FTS temperatures at 87.5 km altitude with 57 coincident nightly averaged temperatures derived from the OH\*(6-2) band at Davis Station, Antarctica ( $68.6^\circ$  S,  $78^\circ$  E) found the ACE-FTS average to be  $\sim 7$  K colder than OH averaged value (Sica et al., 2007). Weighting the ACE-FTS temperatures with a Gaussian centred on 87 km with a half width of 8 km increased the ACE-FTS mean by only 0.3 K. von Savigny et al. (2004) reported a mean temperature difference of 7.1 K between collocated Mesospheric Temperature Mapper and SCIAMACHY observations again with the ground-based values higher than the satellite values.

It appears that temperatures derived from ground-based instruments that record hydroxyl emissions tend to be warmer by  $\sim 5$ – $7$  K than the corresponding values measured by satel-

lites. Atmospheric temperature measurement from OH rotational spectra has always been subject to the twin difficulties of an inexact knowledge of the emission height and the dependence of the retrieved temperature on the rotational transition probabilities used. There have already been several reports of the use of different transition probabilities in order to bring OH rotational temperatures into agreement with other methods (e.g. Turnbull and Lowe, 1989; French et al., 2000). We have examined the impact of the altitude and the thickness of the emission layer on the temperatures in this study, but we have found that it is insufficient to eliminate the difference between satellite and OH rotational temperatures. At this point, we have not been able to identify the exact reason for the discrepancy between satellite and ground-based OH temperatures, and further work will be required to resolve the problem.

## 5 Conclusions

We began this study by making a comparison of OH-equivalent temperatures derived from temperature profiles retrieved by the ACE-FTS satellite with ground based OH\*(3-1) values measured at Maynooth ( $53.2^\circ$  N,  $6.4^\circ$  W) more than a decade earlier. The annual cycle of temperature at mesopause altitudes was well reproduced and excellent agreement was obtained in the absolute value of the

temperature minimum ( $\sim 162$  K) and in its time of occurrence in the cycle. A significant divergence was observed in mid-winter however, with the ACE-FTS OH equivalents more than 20 K less than the ground-based measurements. Results from ground stations at similar latitudes during the same time period appeared to confirm the validity of the OH\*(3-1) data. Lowering the peak altitude of the weighting function used to compute the OH-equivalent temperatures to 84 km in winter-time brought the satellite results to within 14–15 K of the ground-based values. To bring the OH-equivalent temperatures into agreement with the ground-based values in mid-winter, however, required the peak of the weighting function to be placed at an unrealistically low altitude.

We turned to SABER data because this instrument provides a simultaneous measure of the temperature profile and the OH VER profile at  $1.6 \mu\text{m}$ . The OH equivalent temperatures derived from SABER and ACE-FTS were found to be in good agreement. When the SABER OH  $1.6 \mu\text{m}$  VER profile was applied to its corresponding temperature profile, the OH equivalent temperatures became warmer in winter and colder in summer, but with an overall cold bias compared with the OH\*(3-1) temperatures. These changes occurred because the altitude and the width of the OH emission layer exhibits considerable variability on a day to day basis, but with an overall seasonal pattern in which the layer is at a lower altitude in winter and is generally thinner in summer. The higher temperatures in winter were due to primarily to the lower altitude of the OH layer, while the colder summer temperatures were due to a thinner summer OH layer. We are not aware of previous reports of the effect of the layer width on ground-based temperatures.

The OH\*(3-1) temperatures from Maynooth were  $8.6 \pm 0.8$  K warmer than the OH equivalent temperatures from the satellite and had a slight temperature dependence. We found that the variability of the OH layer in its altitude and width did not allow us to accurately reproduce the “true” OH equivalent temperatures from averaged temperature profiles using averaged OH layer altitudes and widths. On the basis of our study of SABER temperature and OH  $1.6 \mu\text{m}$  VER profiles, we believe that any attempt to compare temperatures from satellites with ground based OH temperatures must have altitude information available on the state of the OH layer when the satellite temperature profile was recorded.

OH-equivalent temperatures from ACE-FTS and SABER were compared with OH\*(3-1) rotational temperatures from Wuppertal recorded during the same time period (2004–2005). The general trend of the results found for Maynooth from a decade earlier, were well reproduced in the case of the Wuppertal data, but the magnitude of the warm temperature bias of the ground-based data was reduced to  $4.5 \pm 0.5$  K. A warm bias of temperatures measured by ground based instruments compared with equivalent temperatures derived from satellites has been reported now on a number of occasions. Further work will be required by both the satellite and

ground-based community in order to understand the origin of this discrepancy.

*Acknowledgements.* The Atmospheric Chemistry Experiment (ACE), also known as SCISAT, is a Canadian-led mission mainly supported by the Canadian Space Agency and the Natural Sciences and Engineering Research Council of Canada. We thank the entire ACE-FTS team for the provision of the temperature profiles used in this study. We are especially grateful to P. Bernath, K. Walker, C. Boone and R. J. Sica from the ACE mission team for reading an early version of this manuscript and for providing helpful comments on it. We also thank the SABER/TIMED team for making the SABER data freely available. The use of the CEDAR Data System in providing access to the Stockholm data, and the permission of P. Espy, Norwegian University of Science and Technology (NTNU), Trondheim, Norway, to use it are gratefully acknowledged. A particular word of thanks is due to D. Offermann of the University of Wuppertal, Germany for providing us with the complete set of re-analysed GRIPS data. This work was supported by the Irish Fulbright Commission through a 2007 scholarship, and the Ireland Canada University Foundation through the 2006 Glen Dimplex Scholarship to F. J. Mulligan. R. P. Lowe acknowledges the financial support of the National Science and Engineering Research Council of Canada.

Topical Editor U.-P. Hoppe thanks two anonymous referees for their help in evaluating this paper.

## References

- Baker, D. J. and Stair Jr., A. T.: Rocket measurements of the altitude distributions of the hydroxyl airglow, *Physica Scripta*, 37, 611–622, 1988.
- Beig, G., Keckhut, P., Lowe, R. P., Roble, R. G., Mlynczak, M. G., Scheer, J., Fomichev, V. I., Offermann, D., French, W. J. R., Shepherd, M. G., Semenov, A. I., Remsberg, E. E., She, C. Y., Lübken, F. J., Bremer, J., Clemesha, B. R., Stegman, J., Sigernes, F., and Fadnavis, S.: Review of Mesospheric Temperature Trends, *Rev. Geophys.*, 41(4), 1015, doi:10.1029/2002RG000121, 2003.
- Bernath, P. F., McElroy, C. T., Abrams, M. C., Boone, C. D., Butler, M., Camy-Peyret, C., Carleer, M., Clerbaux, C., Coheur, P.-F., Colin, R., DeCola, P., De Mazière, M., Drummond, J. R., Dufour, D., Evans, W. F. J., Fast, H., Fussen, D., Gilbert, K., Jennings, D. E., Llewellyn, E. J., Lowe, R. P., Mahieu, E., Mc-Connell, J. C., McHugh, M., McLeod, S. D., Michaud, R., Midwinter, C., Nassar, R., Nichitiu, F., Nowlan, C., Rinsland, C. P., Rochon, Y. J., Rowlands, N., Semeniuk, K., Simon, P., Skelton, R., Sloan, J. J., Soucy, M.-A., Strong, K., Tremblay, P., Turnbull, D., Walker, K. A., Walkty, I., Wardle, D. A., Wehrle, V., Zander, R., and Zou, V.: Atmospheric Chemistry Experiment (ACE): Mission overview, *Geophys. Res. Lett.*, 32, L15S01, doi:10.1029/2005GL022386, 2005.
- Bevington, P. R.: Data reduction and error analysis for the physical sciences, McGraw Hill, New York, 1992.
- Bittner, M., Offermann, D., and Graef, H.-H.: Mesopause temperature variability above a midlatitude station in Europe, *J. Geophys. Res.*, 105, 2045–2058, 2000.
- Bittner, M., Offermann, D., Graef, H.-H., Donner, M., and Hamilton, K.: An 18-year time series of OH rotational temperatures

- and middle atmosphere decadal variations, *J. Atmos. Sol. Terr. Phys.*, 64, 1147–1166, 2002.
- Boone, C. D., Nassar, R., Walker, K. A., Rochon, Y., McLeod, S. D., Rinsland, C. P., and Bernath, P. F.: Retrievals for the atmospheric chemistry experiment Fourier-transform spectrometer, *Appl. Optics*, 44(33), 7218–7231, 2005.
- French, W. J. R., Burns, G. B., Finlayson, K., Greet, P. A., Lowe, R. P., and Williams, P. F. B.: Hydroxyl (6,2) airglow emission intensity ratios for rotational temperature determination, *Ann. Geophys.*, 18, 1293–1303, 2000, <http://www.ann-geophys.net/18/1293/2000/>.
- Fritts, D. C., Williams, B. P., She C. Y., Vance, J. D., Rapp, M., Lübken, F.-J., Müllemann, A., Schmidlin, F. J., and Goldberg, R. A.: Observations of Extreme Temperature and Wind Gradients near the Summer Mesopause during the MaCWAVE/MIDAS Rocket Campaign, *Geophys. Res. Lett.*, 31, L24S06, doi:10.1029/2003GL019389, 2004.
- Espy, P. J. and Stegman, J.: Trends and variability of mesospheric temperature at high-latitudes, *Phys. Chem. Earth*, 27, 543–553, 2002.
- Garcia, R. R., Marsh, D. R., Kinnison, D. E., Boville, B. A., and Sassi, F.: Simulation of secular trends in the middle atmosphere, 1950–2003, *J. Geophys. Res.*, 112, D09301, doi:10.1029/2006JD007485, 2007.
- Liu, G. and Shepherd, G. G.: An empirical model for the altitude of the OH nightglow emission, *Geophys. Res. Lett.*, 33, L09805, doi:10.1029/2005GL025297, 2006.
- López-Gonzalez, M. J., García-Comas, M., Rodríguez, E., López-Puertas, M., Shepherd, M. G., Shepherd, G. G., Sargoytchev, S., Aushev, V. M., Smith, S. M., Mlynczak, M. G., Russell, J. M., Brown, S., Cho, Y.-M., and Wiens, R. H.: Ground-based mesospheric temperatures at mid-latitude derived from O<sub>2</sub> and OH airglow SATI data: Comparison with SABER measurements, *J. Atmos. Terr. Phys.*, 69, 2379–2390, doi:10.1016/jastp.2007.07.004, 2007.
- Lowe, R. P., Gilbert, K. L., and Turnbull, D. N.: High-latitude summer observations of the hydroxyl airglow, *Planet. Space Sci.*, 39, 1263–1270, 1991.
- Lowe, R. P.: Correlation of WINDII/UARS airglow emission heights with ground-based rotational temperature measurements, Paper presented at the 22nd European Meeting on Atmospheric Studies by Optical Methods, Nurmijärvi, Finland, 28 August–1 September 1995.
- Marsh, D. R., Garcia, R. R., Kinnison, D. E., Boville, B. A., Sassi, F., Solomon, S. C., and Matthes, K.: Modelling the whole atmosphere response to solar cycle changes in radiative and geomagnetic forcing, *J. Geophys. Res.*, 112, D23306, doi:10.1029/2006JD008306, 2006.
- Makhlouf, U. B., Picard, R. H., and Winick, J. R.: Photochemical-dynamical modelling of the measured response of airglow to gravity waves, *J. Geophys. Res.*, 100, 11 289–11 311, 1995.
- McDade, I. C.: The altitude dependence of the OH ( $X^2\Pi$ ) vibrational distribution in the nightglow: some model expectations, *Planet. Space Sci.*, 39, 1049–1057, 1991.
- McHugh, M., Magill, B., Walker, K. A., Boone, C. D., Bernath, P. F., and Russell III, J. M.: Comparison of atmospheric retrievals from ACE and HALOE, *Geophys. Res. Lett.*, 32, L15S10, doi:10.1029/2005GL022403, 2005.
- Melo, S. M. L., Lowe, R. P., and Russell, J. P.: Double-peaked hydroxyl airglow profiles observed from WINDII/UARS, *J. Geophys. Res.*, 105(D10), 12 397–12 403, 2000.
- Mertens, C. J., Schmidlin, F. J., Goldberg, R. A., Remsberg, E. E., Pesnell, W. D., Russell III, J. M., Mlynczak, M. G., López-Puertas, M., Wintersteiner, P. P., Picard, R. H., Winick, J. R., and Gordley, L. L.: SABER observations of mesospheric temperatures and comparisons with falling sphere measurements taken during the 2002 summer MacWAVE campaign, *Geophys. Res. Lett.*, 31, L03105, doi:10.1029/2003GL018605, 2004.
- Mulligan, F. J., Horgan, D. F., Galligan, J. M., and Griffin, E. M.: Mesopause temperatures and integrated band brightnesses calculated from airglow OH emissions recorded at Maynooth (53.2° N, 6.4° W) during 1993, *J. Atmos. Terr. Phys.*, 57, 1623–1637, 1995.
- Oberheide, J., Offermann, D., Russell III, J. M., and Mlynczak, M. G.: Intercomparison of kinetic temperature from 15  $\mu\text{m}$  CO<sub>2</sub> limb emissions and OH\*(3, 1) rotational temperature in nearly coincident air masses: SABER, GRIPS, *Geophys. Res. Lett.*, 33, L14811, doi:10.1029/2006GL026439, 2006.
- Offermann, D., Jarisch, M., Donner, M., Steinbrecht, W., Semenov, A. I.: OH temperature re-analysis forced by recent variance increases, *J. Atmos. Sol. Terr. Phys.*, 68, 1924–1933, 2006.
- Reed, B. C.: Linear least-squares fits with errors in both coordinates. II: Comments on parameter variances, *Am. J. Phys.*, 60(1), 59–62, 1992.
- Schwartz, M. J., Lambert, A., Manney, G. L., Read, W. G., Livesey, N. J., Froidevaux, L., Ao, C. O., Bernath, P. F., Boone, C. D., Cofield, R. E., Daffer, W. H., Drouin, B. J., Fetzer, E. J., Fuller, R. A., Jarnot, R. F., Jiang, J. H., Jiang, Y. B., Knosp, B. W., Kruger, K., Li, J.-L. F., Mlynczak, M. G., Pawson, S., Russell III, J. M., Santee, M. L., Snyder, W. V., Stek, P. C., Thurstans, R. P., Tompkins, A. M., Wagner, P. A., Walker, K. A., Waters, J. W., and Wu, D. L.: Validation of the Aura Microwave Limb Sounder Temperature and Geopotential Height Measurements, *J. Geophys. Res.*, doi:10.1029/2007JD008783, in press, 2008.
- She, C. Y. and Lowe, R. P.: Seasonal temperature variations in the mesopause region at mid-latitude: comparison of lidar and hydroxyl rotational temperatures using WINDII/UARS OH height profiles, *J. Atmos. Sol. Terr. Phys.*, 60(16), 1573–1583, 1998.
- Sica, R. J., Izawa, M. R. M., Walker, K. A., Boone, C., Petelina, S. V., Argall, P. S., Bernath, P., Burns, G. B., Catoire, V., Collins, R. L., Daffer, W. H., De Clercq, C., Fan, Z. Y., Firanski, B. J., French, W. J. R., Gerard, P., Gerding, M., Granville, J., Innis, J. L., Keckhut, P., Kerzenmacher, T., Klekociuk, A. R., Kyrö, E., Lambert, J. C., Llewellyn, E. J., Manney, G. L., McDermid, I. S., Mizutani, K., Murayama, Y., Piccolo, C., Raspollini, P., Ridolfi, M., Robert, C., Steinbrecht, W., Strawbridge, K. B., Strong, K., Stübi, R., and Thurairajah, B.: Validation of the Atmospheric Chemistry Experiment (ACE) version 2.2 temperature using ground-based and space-borne measurements, *Atmos. Chem. Phys. Discuss.*, 7, 12 463–12 539, 2007.
- Sigernes, F., Shumilov, N., Deehr, C. S., Nielsen, K. P., Svenoe, T., and Havnes, O.: Hydroxyl rotational temperature record from the auroral station in Adventdalen, Svalbard (78N, 15E), *J. Geophys. Res.*, 108(A9), 1342, doi:10.1029/2001JA009023, 2003.
- Sivjee, G. G.: Airglow hydroxyl emissions, *Planet. Space Sci.*, 40, 235–242, 1992.
- Turnbull, D. N. and Lowe, R. P.: Vibrational population distribution in the hydroxyl night airglow, *Can. J. Phys.*, 61, 244–250, 1983.



- Turnbull, D. N. and Lowe, R. P.: New hydroxyl transition probabilities and their importance in airglow studies, *Planet. Space Sci.*, 37, 723–738, 1989.
- von Savigny, C., Eichmann, K.-U., Llewellyn, E. J., Bovensmann, H., Burrows, P. J., Bittner, M., Hoppner, K., Offermann, D., Taylor, M. J., Zhao, Y., Steinbrecht, W., and Winkler, P.: First near-global retrievals of OH rotational temperatures from satellite-based Meinel band emission measurements, *Geophys. Res. Lett.*, 31, L15111, doi:10.1029/2004GL020410, 2004.
- von Zahn, U., Fricke, K. H., Gerndt, R., and Blix, T.: Mesospheric temperatures and the OH layer height as derived from ground-based lidar and OH\* spectrometry, *J. Atmos. Terr. Phys.*, 49, 863–869, 1987.
- von Zahn, U., Höffner, J., Eska V., and Alpers, M.: The mesopause altitude: Only two distinctive levels worldwide?, *Geophys. Res. Lett.*, 23(22), 3231–3234, 1996.
- Zhang, S. P. and Shepherd, G. G.: The influence of the diurnal tide on the O(<sup>1</sup>S) and OH emission rates observed by WINDII on UARS, *Geophys. Res. Lett.*, 26(4), 529–532, 1999.